Custom lifetime phantoms for characterization and benchmarking of a new CAPS fluorescence-lifetime camera

Lapauw, Thomas; Van Den Dries, Thomas; Ingelberts, Hans; Hernot, Sophie; Kuijk, Maarten

Published in:
Advanced Biomedical and Clinical Diagnostic and Surgical Guidance Systems XX

DOI:
10.1117/12.2609545

Publication date:
2022

Document Version:
Final published version

PROCEEDINGS OF SPIE

SPIEDigitalLibrary.org/conference-proceedings-of-spie

Custom lifetime phantoms for characterization and benchmarking of a new CAPS fluorescence-lifetime camera

Lapauw, Thomas, Van den Dries, Thomas, Ingelberts, Hans, Hernot, Sophie, Kuijk, Maarten

Thomas Lapauw, Thomas Van den Dries, Hans Ingelberts, Sophie Hernot, Maarten Kuijk, "Custom lifetime phantoms for characterization and benchmarking of a new CAPS fluorescence-lifetime camera," Proc. SPIE 11949, Advanced Biomedical and Clinical Diagnostic and Surgical Guidance Systems XX, 1194902 (7 March 2022); doi: 10.1117/12.2609545

SPIE.

Event: SPIE BiOS, 2022, San Francisco, California, United States

Custom lifetime phantoms for characterization and benchmarking of a new CAPS fluorescence-lifetime camera

Thomas Lapauw*[a], Thomas Van den Dries[a], Hans Ingelberts[a], Sophie Hernot[b] and Maarten Kuijk[a]
[a]Dept. ETRO, Vrije Universiteit Brussel, Pleinlaan 2, Brussels, Belgium;
[b]Dept. BEFY, ICMI, Vrije Universiteit Brussel, Pleinlaan 2, Brussels, Belgium
* Email: thomas.lapauw@vub.be - http://www.etrovub.be

ABSTRACT

Fluorescence imaging has been used for quite some time in microscopy, preclinical and medical imaging, as well as in other domains. There has been interest in using the time-behaviour of fluorophores to gain additional information. This time-behaviour, called the fluorescence lifetime, is a property of the fluorophore and can also reveal information about its environment through modulation of this lifetime. Fluorescence-lifetime imaging could improve imaging of existing fluorescent contrast agents or could enable novel applications.
The *tau*CAM, based on the Current-assisted photonic sampler (CAPS), is being developed at our research department with the purpose of achieving real-time fluorescence lifetime imaging. Previous versions have already shown some results in doing lifetime imaging through experiments and demonstrations. Elaborate characterisation of its imaging capabilities in this domain has yet to be performed due to the lack of standardisation and phantoms available for lifetime imaging.
In this publication we will discuss the (real-time) lifetime and intensity imaging capabilities of the *tau*CAM, the latest iteration of our CAPS camera, housing a new 64×64-pixel sensor. The groundwork will be laid for the development of phantoms for lifetime imaging based on phantoms made for fluorescence intensity imaging. These will in turn be measured using reference equipment and used to characterize the accuracy and precision of the results from the *tau*CAM.

Keywords: Fluorescence Lifetime, CAPS, preclinical imaging, Time-gated camera, near-infrared

1. INTRODUCTION

In life sciences there is an unending search towards new imaging modalities with the goal of gaining as much useful information from each experiment. These new imaging techniques yield new ways of designing experiments and trying out new approaches. Fluorescence intensity imaging has been used both in microscopy as well as in widefield in-vivo and preclinical imaging. The information gained from intensity imaging can be extended with spectroscopy which uses wavelength to differentiate between fluorophores in the same sample. However, due to tissue absorption and scattering, the useful wavelengths in-vivo are limited to near infrared (NIR). This makes spectral multiplexing options limited due to the narrow bandwidth of the NIR-I band.

Other than wavelength, the distinct time behaviour of the different fluorophores can also be imaged. This technique, called fluorescence lifetime imaging, comes with its own set of challenges. NIR fluorophores usually have lifetimes in the range of a few hundred picoseconds up to two nanoseconds, necessitating specialized imaging equipment[1].

Innovations in technology have allowed for research towards novel applications for fluorescence lifetime[2–9]. In the field of fluorescence intensity, efforts have been made to create phantoms and standardisation techniques[10] however no such work has been done for lifetime imaging. Our team has been developing a real-time widefield camera for fluorescence lifetime with good performance in the NIR-I band, named the *tau*CAM, based on our proprietary CAPS-array image sensor. Though previous experiments have shown promising results, no standardisation and verification has been done. This makes the challenge twofold: evaluate the materials and fluorophores for lifetime phantoms, verify the results using reference equipment and use these results to benchmark the *tau*CAM.

In this work, phantoms developed for fluorescence imaging from other research were translated towards lifetime imaging applications. The phantoms made are early first trials to evaluate viability for the use in characterization of fluorescence lifetime imaging equipment. Multiple different base materials with different concentrations of several fluorophores were

Advanced Biomedical and Clinical Diagnostic and Surgical Guidance Systems XX,
edited by Caroline Boudoux, James W. Tunnell, Proc. of SPIE Vol. 11949,
1194902 · © 2022 SPIE · 1605-7422 · doi: 10.1117/12.2609545

evaluated for the creation of these phantoms. Each material combination is measured using lifetime reference equipment and imaged with the *tau*CAM.

2. CAMERA

The *tau*CAM is a fully integrated CMOS high-speed (sub-)nanosecond time-gated camera with high repetition rate and high quantum efficiency (QE) in NIR. The *tau*CAM is built around the CAPS sensor that manages in pixel gating through modulation of electric fields in the substrate.[11]

A time-gated sensor can be turned *on* and *off* during specific time windows, collecting any signal generated by photons during that time or ignoring it outside that window. More specifically, the CAPS sensor collects the photoelectrons generated by the fluorescent emission incident on the active area, in the detection node in the centre of the pixel. This is done during a specific time window over multiple excitation-emission cycles (coined integration cycles). When enough signal is collected, each pixel can be read out for processing. Any photoelectrons generated by light incident on the sensor outside this window will be discarded. More information about the working of the pixel can be found in earlier publications[4,11].

This windowed integration technique lends itself well for real-time video through lifetime determination techniques using a limited number of windows such as Rapid Lifetime Determination (RLD) and its variants. For more precise measurements and multi-exponential decays, full decay analysis can be done at the penalty of higher acquisition times for additional windows.[4]

Other publications have already demonstrated the time-gating capabilities of earlier generations sensors and hardware[11] as well as real time NIR fluorescence lifetime imaging capabilities[4]. The latest generation sensor is a 64×64-pixel sensor that contains various improvements to increase QE in the gated regime, reduced dark current and sharper instrument response function (IRF)[12].

3. PHANTOMS

To be able to verify the measurements of the *tau*CAM under development, solid references are necessary. However, as mentioned before, no standards for fluorescence lifetime exist so far. Testing the lifetime of different solutions in-vitro has been used before, but this hardly replicates in-vivo environments or realistic applications. For this reason, custom fluorescence lifetime phantoms need to be developed.

3.1 Literature

In this subsection earlier works that cover the creation of fluorescent phantoms will be explored. Most focus will be put on the materials used in the construction: base material, scattering and absorption agents and fluorophores. None of the phantoms listed below are commercially available.

De Grand et al. (2006)[13] developed a tissue-like phantom for NIR fluorescence (NIRF) imaging system assessment and surgeon training. In their publication they use gelatine with TBS as a substrate with bovine hemoglobin and intralipids as absorbing and scattering agents. The fluorescent inclusions are made based on ICG labelled microbeads combined with hydroxyapatite crystals to simulate microcalcifications. The base material of the inclusions is again gelatine combined with the abovementioned constituents. They estimated the contrast agent concentration in cells to be between 160nM and 1µM. The fluorophore concentration in the inclusion used for their demonstration was 1µM ICG equivalence

Pleijhuis et al. (2014)[14] did similar work to *De Grand et al*. in creating a realistic phantom for training and simulation NIRF guided breast cancer surgery. The base material is again TBS based gelatine with bovine hemoglobin and intralipid. To prevent bacterial growth sodium azide was added. The inclusions they created used agarose as base material due to the higher melting point compared to gelatine to prevent melting during casting. Inclusions with 10µM ICG were determined to be optimal.

Akarçay et al. (2012)[15] discuss the optical characterisation of gelatine (16%w/v) based phantoms using titanium dioxide (TiO_2) as the scatterer. For their TiO_2 concentration (1g/L) they measured a reduced scattering concentration of 2.2 cm^{-1}.

Moffit et al. (2006)[16] covers the creation of a polyurethane solid phantom that mimics the optical properties of biologic tissues at different wavelengths. There is no fluorescence present however they investigate in depth on how to recreate the optical properties in polyurethane. They use TiO_2as a scattering agent and a combination of two optical dyes to create a

specific absorption spectrum. Epoxy resin was also tried, however, in their experiments the absorption of the dyes was lost during curing.

Gorpas et al. (2019)[10,17,18] present their latest iteration of their phantom for benchmarking fluorescence imaging systems. Their approach consists of making a solid phantom using casted polyurethane resin combined with machining steps. The scattering and absorbing agents are TiO_2 and bovine hemin respectively. For the background absorption of the main bulk of the phantom, nigrosin is used. Quantum dots (Qdots) are used as fluorophore. The fabrication of the phantom is a multistep process to create a standardized phantom that can assess multiple different parameters of an imaging system.

Ruiz et al. (2020)[19] based their phantom on the work of *Gorpas et al*. similarly they use polyurethane resin as material in addition to a 3D printed base. The 3D printed base serves as a mould for the fluorescent resin mixture. The goal of *Ruiz et al.* was to make an ICG equivalent fluorescence standard. The ICG concentrations used range from 1000 nM down to 0 nM (in approximately 1/3 dilutions over 8 wells with the last being 0 nM).

The goal of the first two is to achieve a realistic phantom that can be used for imaging system assessment. Gelatine has been shown to be a good option for a base material. It will provide an aqueous environment similar to in-vivo conditions. Extrapolating the parameters of the fluorophore to the specifications from literature (in aqueous solution) is realistic. However, evaporation when exposed to air and bacterial growth might limit the amount of time it can be stored.

Resin based phantoms provide more robustness and long-term stability due to being completely solid rather than gel. But the environment that they provide to the fluorophore is unlike any in-vivo environment. Long term stability could be increased, however any other parameter such as spectra, quantum yield, lifetime, etc. will need to be measured objectively to provide a reference.

3.2 Phantom specifications

For the phantoms in this work, different approaches will be taken by combining different elements from the publications listed in the previous section. The main parameters to benchmark in a lifetime imaging system include accuracy and precision of the lifetime determination for different concentrations and intensity, homogeneity of the image and multiplexing capabilities. To create phantoms that are usable to assess these parameters, a few requirements need to be set:

- Solid or gel material
- Optical properties (absorption and scattering) matching tissue
- Fluorophore concentration(s) representative of what can be expected in-vivo
- Usage of multiple different fluorophores with distinct lifetimes but similar spectra (within or between phantoms)

The two most common base materials from section 3.1 are gelatine and polyurethane. Agarose is also used as a base material as alternative to gelatine. For a solid phantom, epoxy resin can possibly be used as an alternative to polyurethane, but earlier studies suggest incompatibility with certain (non-fluorescent) dyes during curing.[16]

To imitate the appropriate optical properties (mainly absorption and scattering) different constituents can be used. As scatterers, most mentioned are titanium dioxide and intralipid. Other candidates are aluminium oxide, SiO_2, polyester, latex microspheres[16]. The absorber of choice in gelatine phantoms is bovine hemoglobin, while for solid phantoms this is replaced by hemin, ink, or dye.

Most phantoms use ICG as fluorophore; additionally, ICG is currently the only medically approved NIR fluorescent dye for in-vivo use. This makes ICG a good candidate for the creation of a fluorescence lifetime phantom. Although the lifetime in an aqueous environment is quite short, earlier experiments have shown that it is not outside of the capabilities of the *tau*CAM. Additionally, more and more NIR dyes are researched and developed for in-vivo use. Some examples of dyes currently under research for in-vivo applications are: IRdye800CW, BLZ-100, SGM-101[20], s775z [21] and FNIR[22].

In *Gorpas et al.* Qdots are used for their improved photostability and absence of quenching in solid phantoms. Qdots exhibit lifetimes of multiple orders of magnitudes longer (tens of nanoseconds) than most NIR dyes (hundreds of picoseconds)[1,23]. This makes them unsuitable for lifetime phantoms that mimic in-vivo conditions of NIR fluorophores.

3.3 Phantom creation

In this work three different phantoms were created and tested: one based on *gelatine*, another based on *polyurethane*, and one based on *epoxy*. Each of these was made with nine wells which contain a dilution series starting at 2050 nM down to 8 nM (½ dilution between wells, see Table 1). And this was repeated for 3 different fluorophores with a distinct lifetime but with an overlapping excitation and emission spectrum: ICG*, IRDye800CW† and s775z. These three are all cyanine dyes that have an absorption and emission spectrum in NIR.

Table 1. Fluorophore concentrations per well

Well	*Concentration (nM)*
1	2050
2	1025
3	512
4	256
5	128
6	64
7	32
8	16
9	8

Figure 1. Finished phantom with all wells filled with resin

The range of concentrations were decided upon from earlier experiments matched to what would be relevant in-vivo. These concentrations are lower than what is used in *Pleihuijs et al.* but higher than *Ruiz et al.* Fluorophores dissolved in DMSO were added in a 50 µL quantity for a preparation volume of 6 ml of each well. The initial dilution was made to reflect this last step.

Titanium dioxide (Amertek) and hemin (Sigma-Aldrich) are used as scattering and absorbing agents for all three phantoms. Although for the gelatine phantom, using hemoglobin and intralipid would increase realism, imitating optical properties takes precedence since we are using it to assess imaging capabilities. Using similar composition will also improve consistency with respect to the other two solid phantoms.

For the polyurethane phantoms, TiO_2 and hemin were added in the 0.66 mg/g and 0.04 mg/g concentrations respectively. In polyurethane this should result in a corresponding reduced scattering coefficient (μ_s') of 7 cm^{-1} and absorption coefficient (μ_a) of 0.25 cm^{-1}.[10] These values should roughly correspond to the absorption and scattering coefficients of skin tissue at 800 nm[24].

In gelatine the TiO_2 concentration was decided to be 1 mg/g. According to *Akarçay et al.* this results in a reduced scattering coefficient (μ_s') of 2,2 cm^{-1}. For hemin as absorption agent in gelatine no reference in literature was found, hence the same value of 0.04 mg/g was taken. However, for full characterisation reference measurements should be taken.

For the base it was chosen to use black POM (also known as polyacetal or Delrin). POM exhibits strong mechanical, thermal, and chemical stability in addition to being easily machinable. Each base measures 70 mm by 70 mm by 20 mm, 9 circular (ø12 mm, 12 mm depth) wells are milled; in addition, three smaller wells on the corners are milled for orientation (not used here). The 9 circular wells are filled with the different concentrations.

For each base material at least 200 mL was created with the absorbers and scatterers. This was done for both practical reasons and to have adequate quantities for reference. The preparation steps for each phantom can be found below.

* Exciton IR-125
† Li-Cor IRDye 800CW Maleimide

Gelatine phantom procedure

1. Create gelatine mixture: heat 200 mL of aqueous solvent of choice (TBS/PBS/H_2O) to 60 °C. Add 40 g gelatine for a ratio of 16 %w/w. Add 240 mg TiO_2 and 4.8 mg hemin. Mix until completely dissolved using a stirring plate, keep at the same temperature during this process. Sonicating in between stirring steps can help dissolve the TiO_2.
2. Cool down the mixture to 35-40 °C (higher temperatures reduce final fluorescence). For each well measure 6 mL and add 50 µL of the respective fluorophore dilution. Mix well and pour the appropriate quantity in the well. Multiple degassing and sonicating cycles can be done to reduce the bubbles inside of the gelatine

Polyurethane phantom procedure

The polyurethane used is Smooth-On Crystal Clear 204. This needs to be mixed in a 100/90 by weight ratio (A/B).

1. Start with taking 100 g of component A, add 125 mg TiO_2 and 3.8mg Hemin. Mix until completely dissolved using a stirring plate. Sonicating in between stirring steps can help dissolve the TiO_2.
2. For each well measure 3,27 g of component A in a small container. Add 50 µL of the respective fluorophore dilution and mix well. Optionally degassing can be done at this step.
3. Add 2,98 g of the component B mixture to each container and stir well.
4. Degas the containers. Sonicate afterwards to break the surfaced bubbles.
5. Carefully pour the appropriate quantity into wells and degas the phantoms one last time.

Epoxy phantom procedure

The epoxy resin used is unbranded resin[‡]. This needs to be mixed in a 2/1 by weight ratio (resin/hardener).

1. Start with preparing the resin: take 140 g of resin, add 138.6 mg TiO_2 and 4.2 mg hemin and stir with a stirring plate until fully mixed. Sonicating in between stirring steps can help dissolve the TiO_2. Optionally degassing can be done after this step.
2. For each well, measure 4.34 g of resin in a small cup. Add 50 µL of the respective fluorophore dilution and mix well.
3. Degas the resin well. Optionally sonicate to break the bubbles brought to the surface
4. Add 2.17 g of hardener to the mixture to each container and stir well.
5. Degas the mixture well and sonicate to break the bubbles brought to the surface
6. Carefully pour the appropriate quantity into wells and degas the phantoms one last time.

4. MEASUREMENT SETUP & METHODOLOGY

The goal that we want to achieve is to create phantoms that can be used to characterize the lifetime behaviour of the *tau*CAM. To be able to use the created phantoms for our widefield camera the phantoms themselves need to be characterized first. During the creation of the phantoms, larger than necessary quantities of material for each well were made. This excess was poured into labelled cuvettes for use in the reference equipment.

4.1 Reference measurements

For the reference measurements a Mini-τ (Edinburgh Instruments) with the built in Hamamatsu PMT (H10720-01) was used. The excitation source used is an NKT Super-K supercontinuum pulsed laser with a VARIA tuneable optical filter. The excitation wavelength is set to 765 nm ±5 nm. The emission filter is a Semrock BrightLine 819/44 nm bandpass filter.

The Mini-τ uses Time-Correlated Single Photon Counting (TCSPC), lifetime determination is done through curve fitting (Marquardt-Levenberg) in the included software.[25]. Fitting was done using a tail fit with the starting bin deep enough into the decay such that the deviation caused by the IRF would be minimized.

[‡] From the datasheet:
Resin: Bisphenol-A + Bisphenol-F with C12~C14 aliphatic glycidyl ester. (1120g/L)
Hardener: nonylphenol-free cyclo-aliphatic amine (1020g/L)

4.2 *tau*CAM measurement setup

For a widefield setup, an illumination source with high power is necessary since the power is spread out over a larger surface area. For the illumination, an NKT Katana HP 775 nm laser is used (40 Mhz repetion rate). The light from the collimator is coupled into a 200 µm optical fibre which goes to a beam expander (Thorlabs GBE02-B) and engineered diffuser (Thorlabs ED1-S20-MD) to illuminate the field of view. The *tau*CAM is mounted on a vertical rail to adjust the distance to the object. The lens used is a fixed focus lens (Edmund 67714) with an emission bandpass filter mounted in front (Semrock brightline 835/70).

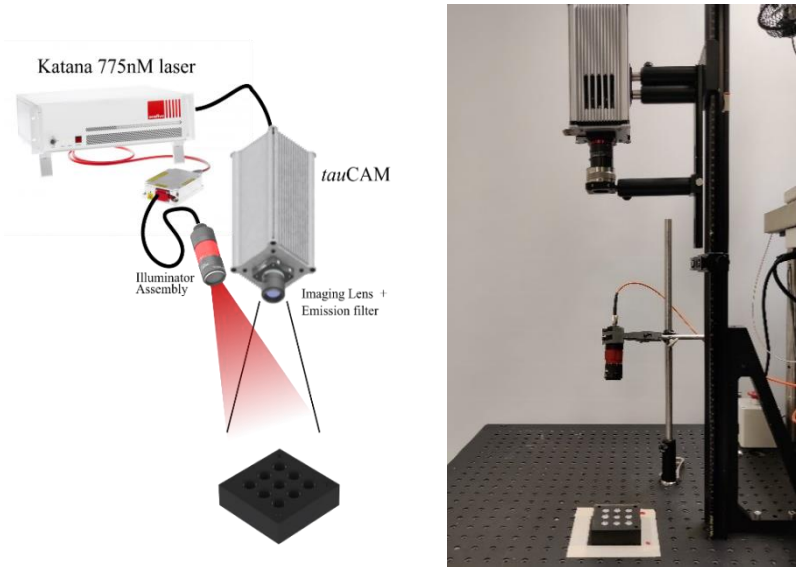

Figure 2. Illustration and picture of the setup

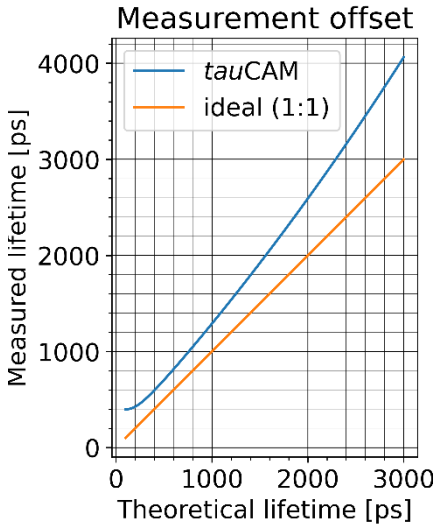

Figure 3. Plot of the *tau*CAM measurement offset

The lifetime determination for the *tau*CAM was done using Rapid Lifetime Determination (RLD) with background subtraction in our own internal testing software. RLD is currently viewed as the most viable option to achieve real-time lifetime video, especially at growing resolutions. This is mainly due to the limited number of time-gated sub-frames required to construct a lifetime image: two frames during the decay and one frame outside to subtract the background from the two others. The computational complexity of the calculations for RLD is low at a trade-off with regards to accuracy and noise-immunity, especially for regions with low SNR.

One major disadvantage is that the influence of the IRF is not negligible especially for shorter lifetimes and for low intensities. This introduces a shift in the calculated lifetime and should be accounted for. However, this compensation is dependent on multiple factors: IRF, actual window positions and background signal. Figure 3 shows a simulation of the measurement offset for different lifetimes, it is based on the IRF of one single pixel and one set of window widths (4 ns) and positions. The orange curve is the ideal situation and the blue one shows the behavior of the *tau*CAM. The *tau*CAM measurements are near-linearly proportional to the actual lifetimes, showing good lifetime sensitivity down to ~200 ps, albeit with an upward offset.

Due to process variation between pixels and signal distribution on the sensor array, the IRF can slightly vary from pixel to pixel. This exacerbates the complexity of the compensation. These non-idealities are also a contributor to the fixed pattern noise of the image and are not yet compensated for.

5. RESULTS

In the previous sections, the creation of the phantoms and the measurement setups were discussed. The cuvettes with the excess material were measured using the Mini-τ for reference and the phantoms themselves were imaged with the *tau*CAM.

Each of the graphs in this section show the lifetime in function of concentration on a $\log_2$ scale to match the ½ dilution series.

The processing of the 2D images of the *tau*CAM was done as follows: the lifetime tiff image is acquired after RLD. Pixels with a valid lifetime are represented by the lifetime in picoseconds, the pixels with invalid lifetime (according to the thresholds in the processing pipeline) are set to zero. This data is in turn processed in Matlab to obtain one single value for the lifetime. Each image is split into nine equal sub-images containing each one well. For each sub-image, the mean of the non-zero pixels is taken as the lifetime value for that well.

The finite dynamic range of the camera forces a compromise between having saturation for the pixels of the highest wells or increasing the integration cycles to have adequate SNR for the lowest wells. The lifetime values for the *tau*CAM measurements are obtained with a single RLD window placement (3 frames) and an acquisition time time chosen to have the brightest pixels not saturated. For lower concentrations, these settings lead to insufficient SNR for consistent lifetime determination which is why they are filtered out. In such cases averaging can be applied while still yielding real-time imaging.[4] Additionally, increasing the integration time aids in collecting enough signal in the lowest concentration regions at the compromise of not being able to apply RLD to saturated regions.

The measurements were done on the fully integrated air-cooled prototype of the *tau*CAM. The sensor runs at 50°C which causes a high contribution to the dark signal, reducing the dynamic range. The sensor for the water-cooled version runs at 20°C and has a dark noise that is more than 10 times lower but was not yet available at the time of the experiments[12].

5.1 Gelatine phantom

Figure 4 shows the measured lifetimes of ICG in gelatine. The lifetimes are short (sub-nanosecond) and are in the same order of magnitude as the values from literature. Fluorescence lifetime is considered independent of the intensity, however at higher concentrations interactions with the environment can influence the lifetime. This can be seen on Figure 4, the lifetime becomes shorter towards higher concentrations. The lifetimes measured with the *tau*CAM are not compensated for the IRF yet. This introduces a clear upwards shift in the lifetimes.

From Figure 4 (b) it can be seen that the lifetime measurements for IRDye800CW are more consistent in comparison to ICG. The fluorescence lifetime stays constant over the whole series of dilutions. Due to the higher emission intensity in comparison to ICG, the *tau*CAM can measure lifetime for more wells.

Not a lot of information is available about s775z, since it is a recently developed fluorophore. No publications list a reference value for the lifetime of s775z. Similar to IRDye800CW the lifetime remains constant over the whole dilution series. s775z is the brightest of the three and ICG has the lowest intensity for the same concentrations.

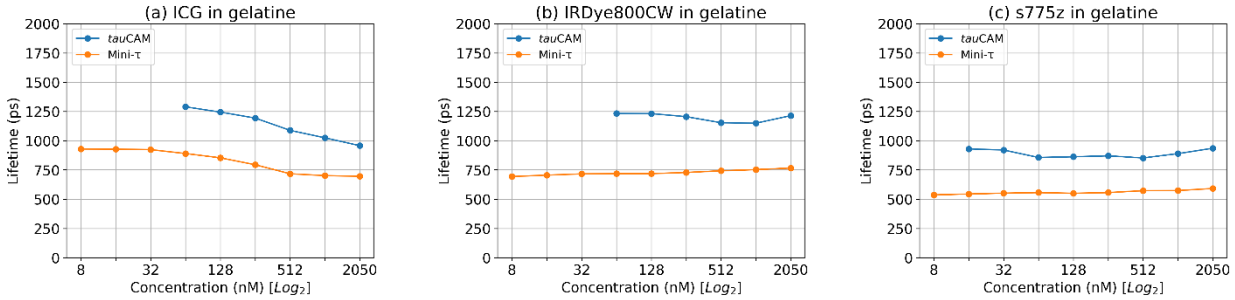

Figure 4. Lifetime in function of concentration for gelatine phantoms. (a) ICG, (b) IRDye800CW, (c) s775z

Figure 5 shows a comparison plot of the lifetimes of the different fluorophores in function of the concentrations measured with the Mini-τ and the *tau*CAM respectively. The fact that ICG demonstrates dependency on its concentration in gelatine, contrary to what is known in theory, will need further investigation.

The gelatine phantom is considered closest to in-vivo conditions once the quantities of TiO_2 and hemin are finetuned to match tissue. In this case deionized water was used for the creation of the gelatine. PBS or TBS could be used to mimic the environment better. Additionally, as done in *Pleijhuis et al.*[14] and *De Grand et al.*[13], bovine hemoglobin and intralipid can be used for added realism.

Another advantage of the gelatine phantom is that the fabrication process is simple and fast, but this contrasts with the time the phantom remains usable. The main limits to this are evaporation and bacterial or fungal growth.

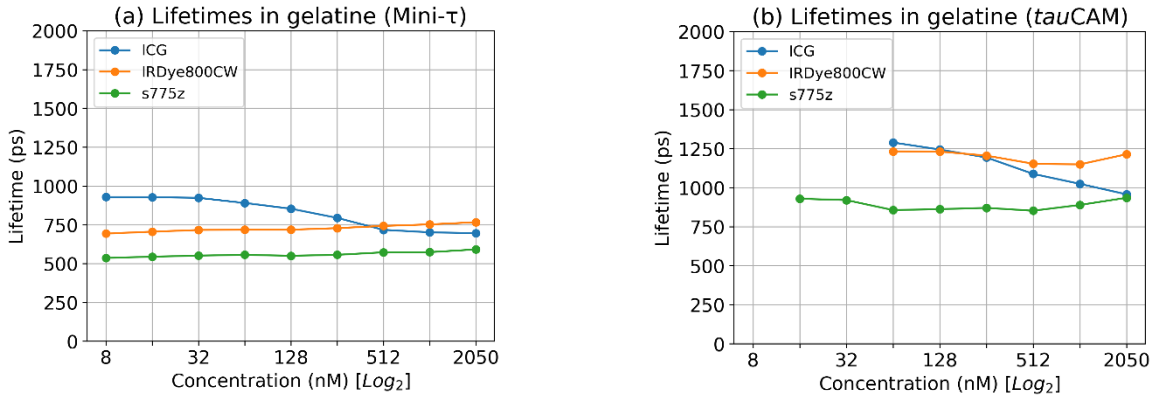

Figure 5. Comparison of lifetimes in gelatine measured with the mini-τ (a) and *tau*CAM (b)

5.2 Polyurethane phantom

From the literature section it becomes clear that most solid phantoms use polyurethane (PU) as a base material. The main advantage of solid resin-based phantoms is that mechanical and chemical stability after curing should be better.

The curves from ICG in PU exhibit a clear trend of rising lifetime with rising concentration (Figure 6). The trend here is opposite to what can be seen in gelatine. The measurements of the Mini-τ show that the lifetime for the lowest six concentrations remains consistent but starting at 512 nM and above the lifetime rises sharply. One hypothesis for this is that the lower concentrations result in a chemical reaction or the fluorophore binding to the resin, resulting in a shorter lifetime. For higher concentrations the amount of free fluorophore molecules becomes prevalent resulting in a sudden rise of lifetime.

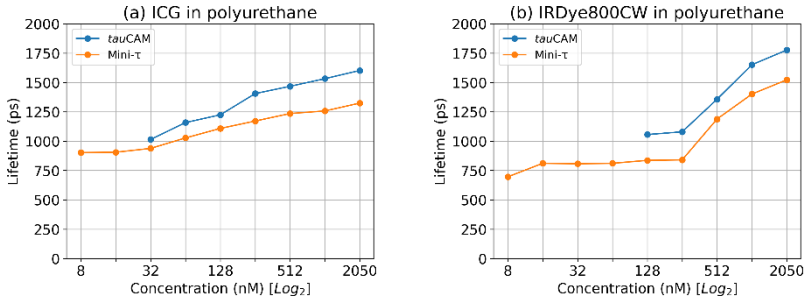

Figure 6. Lifetime in function of concentration for polyurethane phantoms. (a) ICG, (b) IRDye800CW

The polyurethane phantom that uses s775z shows little to no fluorescence after curing the resin, hence the results are omitted. This suggests s775z might be unusable for this kind of phantom. However, during these trials only one phantom with a s775z – PU combination was fabricated so further research is necessary.

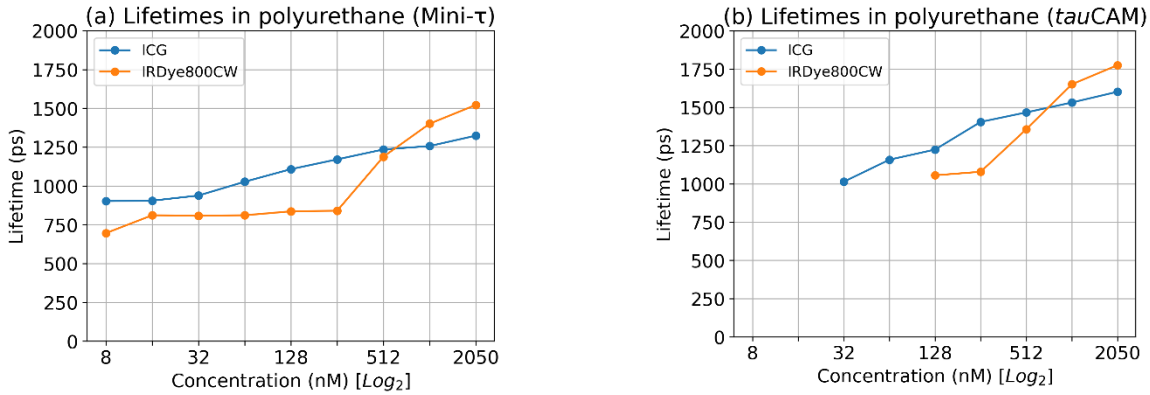

Figure 7. Comparison of lifetimes in polyurethane measured with the mini-τ (a) and *tau*CAM (b) (s775z is omitted)

Although most solid phantoms made for fluorescence imaging use polyurethane as a base material, is does not seem to be as straightforward for lifetime imaging. ICG behaves in a straightforward fashion, exhibiting a rising lifetime with rising concentration. This is clearly not the case for IRDye800CW and s775z where the former has a sudden spike in lifetime and the latter barely shows fluorescence anymore.

5.3 Epoxy phantom

An alternative for polyurethane resin is epoxy resin. In *Moffit et al.*[16] epoxy was unsuccessfully tried as base material to make phantoms with a specific absorption spectrum. Initial experiments showed compatibility between epoxy, DMSO and ICG. From the results on Figure 8 it can be seen that lifetime is not constant with changes in concentration, but the effect is less pronounced in comparison to polyurethane. IRDye800CW shows a similar slope as well as s775z

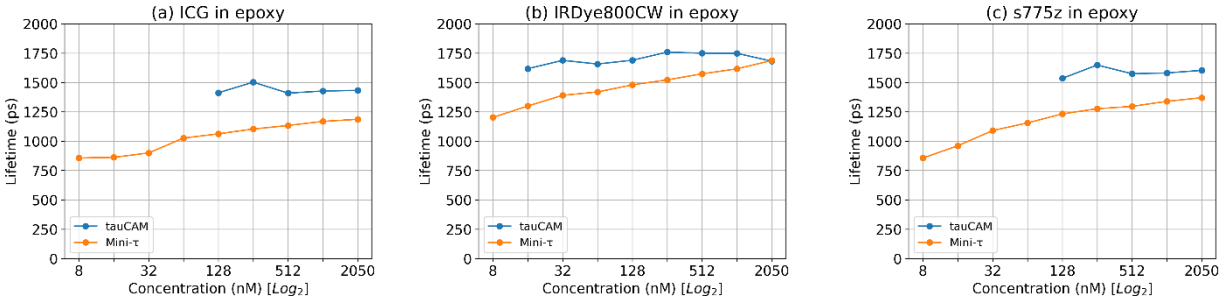

Figure 8. Lifetime in function of concentration for epoxy phantoms. (a) ICG, (b) IRDye800CW, (c) s775z

Epoxy shows promise as a base material for fluorescent lifetime phantoms. Fluorescence is kept after curing; however, the lifetime becomes a longer by a few hundreds of picoseconds in comparison to aqueous conditions. Longer lifetimes decrease the harsh demands of a measurement system, and they reflect the in-vivo conditions less. Another clear disadvantage of epoxy is that the lifetime decreases with decreasing concentration. This prevents consistent lifetime determination for different concentrations. But from the fact that the curves on Figure 9 are parallel, discrimination based on lifetime remains possible over a large range of concentrations.

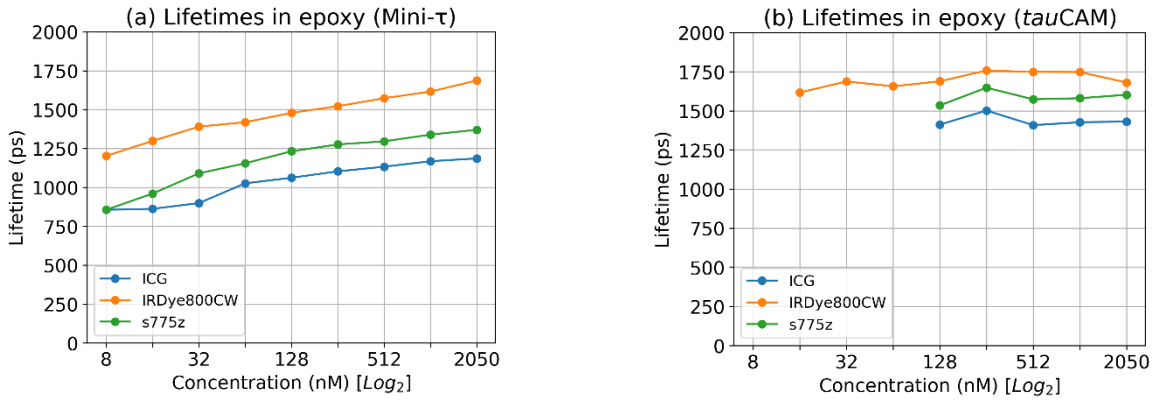

Figure 9. Comparison of lifetimes in epoxy measured with the mini-τ (a) and *tau*CAM (b)

5.4 Lifetime imaging with the *tau*CAM

From the previous section, the *tau*CAM in combination with the current processing pipeline is able to measure lifetime with adequate precision to distinguish fluorophores with different lifetimes. Figure 10 shows the discrimination capabilities of widefield lifetime imaging. The highest concentration wells of ICG and IRDye800CW in epoxy are put together in one image. From the intensity image it is not possible to discriminate the different fluorophores. But using time resolved fluorescence imaging, the *tau*CAM can create contrast based on lifetime. The orange wells correspond to longer lifetimes which corresponds to IRDye800CW, the green wells correspond to ICG with a shorter lifetime. This image was made with 1e6 repetitions and a window width of 4 ns. Each of the three RLD windows was measured 5 times and averaged before calculating the lifetime.

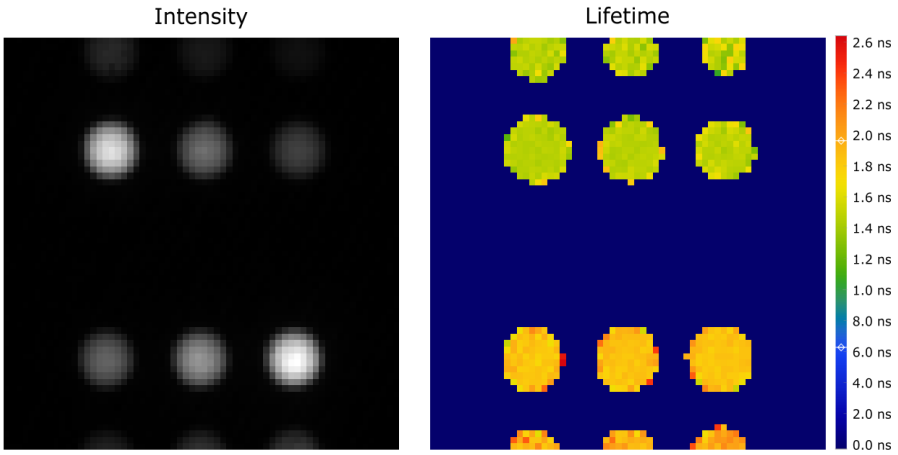

Figure 10. Intensity and lifetime image of ICG and IRDye800CW in epoxy imaged with the tauCAM.

At the beginning of this section the finite dynamic range of the sensor and the limitations it imposes on the lifetime determination for low intensities were discussed. Figure 11 shows an example of a lifetime image created through averaging the sub-frames respectively before calculating the lifetime with RLD. After averaging the lifetime of lowest concentrations can still be measured but with lower uniformity. Without averaging a framerate of 12 frames per second is still achievable, however with averaging this is reduced to only 2 per second.

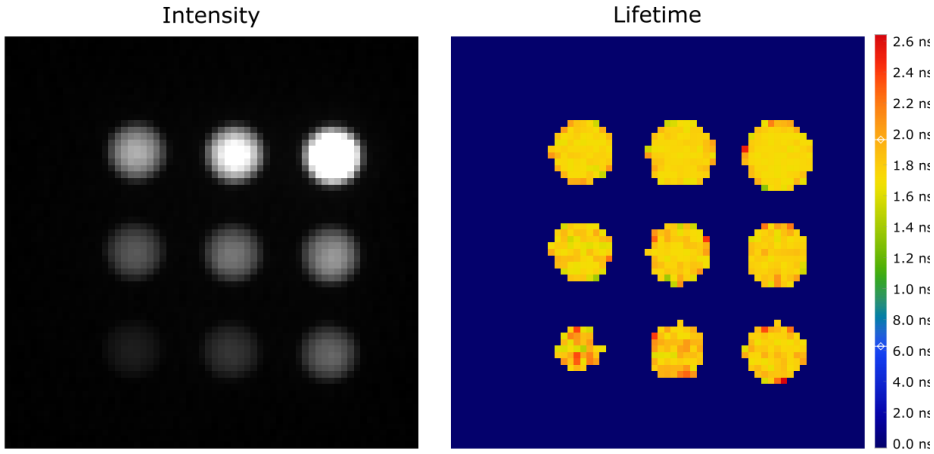

Figure 11. IRDye800CW in epoxy imaged with the *tau*CAM and each sub-frame averaged over 5 measurements

6. REVIEW & CONCLUSION

The work described in this paper is twofold: exploring options with regards to solid and gel-based phantoms for fluorescence lifetime imaging, and at the same time using the results from those to assess the lifetime imaging capabilities of the *tau*CAM by comparing the results to reference measurements.

Gelatine phantoms yield results that correspond closest to reality. The fluorophores used demonstrate the behaviour expected from aqueous environments: sub-nanosecond lifetimes that remain mostly constant over the whole range of concentrations. However, due to these phantoms being water-based, stability and resistance to evaporation remain issues.

Resin phantoms don't experience the evaporation and bacterial growth problem that can occur with gelatine phantoms. Polyurethane is used for fluorescence imaging phantoms with both ICG and Qdots, however these experiments have shown that the performance will depend on the fluorophore used. Additionally, the measured lifetimes show dependency on the concentration. Epoxy phantoms on the other hand demonstrate better compatibility with s775z and the lifetime behaviour for the three fluorophores is linear albeit not fully constant over the range of concentrations. This change in lifetime with changing concentration is something that will need to be investigated.

For all the phantoms it has been shown that the *tau*CAM can image fluorescence lifetime. However due to the limited dynamic range of the current CAPS-sensor determining the lifetime of all concentrations at the same time using the RLD method is challenging. Averaging multiple frames and different lifetime determination methods that use more windows can remedy this in exchange for framerate.

The influence of the IRF of the *tau*CAM is non-negligible for the RLD method. This is clearly shown in the upwards offset of the lifetimes in comparison to the reference measurements. This offset depends on the IRF and RLD settings and will be corrected for in future work by the implementation of suitable algorithms or neural networks. Even without compensation, contrast can be added to homo-spectral fluorophores as an extra source of information that remains invisible with spectroscopy or intensity imaging.

ACKNOWLEDGEMENTS

This work was supported in part by Innoviris, the Brussels Institute for the encouragement of scientific research and innovation, by the Research Council of the Vrije Universiteit Brussel (SRP 19) and by Fonds Wetenschappelijk Onderzoek Vlaanderen (FWOAL920).

REFERENCES

[1] Gioux, S., Lomnes, S.J., Choi, H.S., and Frangioni, J. v., "Low-frequency wide-field fluorescence lifetime imaging using a high-power near-infrared light-emitting diode light source," Journal of Biomedical Optics 15(2), 026005 (2010).

[2] Reichert, D., Erkkilä, M.T., Holst, G., Hecker-Denschlag, N., Wilzbach, M., Hauger, C., Drexler, W., Gesperger, J., Kiesel, B., et al., "Towards real-time wide-field fluorescence lifetime imaging of 5-ALA labeled brain tumors with multi-tap CMOS cameras," Biomedical Optics Express 11(3), 1598 (2020).

[3] Yang, W., and Chen, S.-L., "Time-gated fluorescence imaging: Advances in technology and biological applications," Journal of Innovative Optical Health Sciences 13(03), 2030006 (2020).

[4] Ingelberts, H., Lapauw, T., Debie, P., Hernot, S., and Kuijk, M., "A proof-of-concept fluorescence lifetime camera based on a novel gated image sensor for fluorescence-guided surgery," in Molecular-Guided Surgery: Molecules, Devices, and Applications V, B. W. Pogue and S. Gioux, Eds., 12 (2019).

[5] Sauer, L., "Review of clinical approaches in fluorescence lifetime imaging ophthalmoscopy," Journal of Biomedical Optics 23(09), 1 (2018).

[6] Datta, R., Heaster, T.M., Sharick, J.T., Gillette, A.A., and Skala, M.C., "Fluorescence lifetime imaging microscopy: fundamentals and advances in instrumentation, analysis, and applications," Journal of Biomedical Optics 25(07), 1 (2020).

[7] Powolny, F., Homicsko, K., Sinisi, R., Bruschini, C.E., Grigoriev, E., Homulle, H., Prior, J.O., Hanahan, D., Dubikovskaya, E., et al., "Time-resolved imaging system for fluorescence-guided surgery with lifetime imaging capability," 8 May 2014, 912938.

[8] Kumar, A.T.N., Carp, S.A., Yang, J., Ross, A., Medarova, Z., and Ran, C., "Fluorescence lifetime-based contrast enhancement of indocyanine green-labeled tumors," Journal of Biomedical Optics 22(4), 040501 (2017).

[9] Berezin, M.Y., Guo, K., Akers, W., Northdurft, R.E., Culver, J.P., Teng, B., Vasalatiy, O., Barbacow, K., Gandjbakhche, A., et al., "Near-Infrared Fluorescence Lifetime pH-Sensitive Probes," Biophysical Journal 100(8), 2063–2072 (2011).

[10] Gorpas, D., Koch, M., Anastasopoulou, M., Bozhko, D., Klemm, U., Nieberler, M., and Ntziachristos, V., "Multi-Parametric Standardization of Fluorescence Imaging Systems Based on a Composite Phantom," IEEE Transactions on Biomedical Engineering 67(1), 185–192 (2020).

[11] Lapauw, T., Ingelberts, H., van den Dries, T., and Kuijk, M., "Sub-nanosecond time-gated camera based on a novel current-assisted CMOS image sensor," in Photonic Instrumentation Engineering VI, Y. G. Soskind, Ed., 5 (2019).

[12] van den Dries, T., Lapauw, T., Jegannathan, G., Ingelberts, H., and Kuijk, M., "Submitted to SPIE Photonics West 2022: Compact sub-nanosecond time-gated camera based on a new 64x64 Curre nt-Assisted Photonic Sampler (CAPS) sensor with improved quantum efficiency," in Silicon Photonics XVII (2022).

[13] de Grand, A.M., Lomnes, S.J., Lee, D.S., Pietrzykowski, M., Ohnishi, S., Morgan, T.G., Gogbashian, A., Laurence, R.G., and Frangioni, J. v., "Tissue-like phantoms for near-infrared fluorescence imaging system assessment and the training of surgeons," Journal of Biomedical Optics 11(1), 014007 (2006).

[14] Pleijhuis, R.G., Langhout, G.C., Helfrich, W., Themelis, G., Sarantopoulos, A., Crane, L.M.A., Harlaar, N.J., de Jong, J.S., Ntziachristos, V., et al., "Near-infrared fluorescence (NIRF) imaging in breast-conserving surgery: Assessing intraoperative techniques in tissue-simulating breast phantoms," European Journal of Surgical Oncology 37(1), 32–39 (2011).

[15] Akarçay, H.G., Preisser, S., Frenz, M., and Rička, J., "Determining the optical properties of a gelatin-TiO_2 phantom at 780 nm," Biomedical Optics Express 3(3), 418 (2012).

[16] Moffitt, T., Chen, Y.-C., and Prahl, S.A., "Preparation and characterization of polyurethane optical phantoms," Journal of Biomedical Optics 11(4), 041103 (2006).

[17] Gorpas, D., Koch, M., Anastasopoulou, M., Klemm, U., and Ntziachristos, V., "Benchmarking of fluorescence cameras through the use of a composite phantom," Journal of Biomedical Optics 22(1), 016009 (2017).

[18] Anastasopoulou, M., Koch, M., Gorpas, D., Karlas, A., Klemm, U., Garcia-Allende, P.B., and Ntziachristos, V., "Comprehensive phantom for interventional fluorescence molecular imaging," Journal of Biomedical Optics 21(9), 091309 (2016).

[19] Ruiz, A.J., Wu, M., LaRochelle, E.P.M., Gorpas, D., Ntziachristos, V., Pfefer, T.J., and Pogue, B.W., "Indocyanine green matching phantom for fluorescence-guided surgery imaging system characterization and performance assessment," Journal of Biomedical Optics 25(05), 1 (2020).

[20] Hernot, S., van Manen, L., Debie, P., Mieog, J.S.D., and Vahrmeijer, A.L., "Latest developments in molecular tracers for fluorescence image-guided cancer surgery," in The Lancet Oncology 20(7), Lancet Publishing Group, pp. e354–e367 (2019).
[21] Gamage, R.S., Li, D.-H., Schreiber, C.L., and Smith, B.D., "Comparison of cRGDfK Peptide Probes with Appended Shielded Heptamethine Cyanine Dye (s775z) for Near Infrared Fluorescence Imaging of Cancer," ACS Omega 6(44), 30130–30139 (2021).
[22] Luciano, M.P., Crooke, S.N., Nourian, S., Dingle, I., Nani, R.R., Kline, G., Patel, N.L., Robinson, C.M., Difilippantonio, S., et al., "A Nonaggregating Heptamethine Cyanine for Building Brighter Labeled Biomolecules," ACS Chemical Biology 14(5), 934–940 (2019).
[23] Gaigalas, A.K., DeRose, P., Wang, L., and Zhang, Y.-Z., "Optical Properties of CdSe/ZnS Nanocrystals," Journal of Research of the National Institute of Standards and Technology 119, 610 (2014).
[24] Sandell, J.L., and Zhu, T.C., "A review of in-vivo optical properties of human tissues and its impact on PDT" (2011).
[25] Edinburgh Instruments Ltd., "mini-τ User Guide" (2017).